Translational Oncology
www.transonc.com

Volume 11 Number 2 April 2018 pp. 292–299 292

The Epithelial Sodium Channel (αENaC) Is a Downstream Therapeutic Target of ASCL1 in Pulmonary Neuroendocrine Tumors

Min He[*], Shanshan Liu[†], Sachith Gallolu Kankanamalage[*], Mark D. Borromeo[‡], Luc Girard[*,†], Adi F. Gazdar[†,§,¶], John D. Minna[*,†,§], Jane E. Johnson[*,‡] and Melanie H. Cobb[*]

[*]Department of Pharmacology, University of Texas Southwestern Medical Center, Dallas, Texas; [†]Hamon Center for Therapeutic Oncology Research, University of Texas Southwestern Medical Center, Dallas, Texas; [‡]Department of Neuroscience, University of Texas Southwestern Medical Center, Dallas, Texas; [§]Department of Internal Medicine, University of Texas Southwestern Medical Center, Dallas, Texas; [¶]Department of Pathology, University of Texas Southwestern Medical Center, Dallas, Texas

Abstract

Small cell lung cancer (SCLC) is an aggressive neuroendocrine carcinoma, designated as a recalcitrant cancer by the National Cancer Institute, in urgent need of new rational therapeutic targets. Previous studies have determined that the basic helix-loop-helix transcription factor achaete-scute homolog 1 (ASCL1) is essential for the survival and progression of a fraction of pulmonary neuroendocrine cancer cells, which include both SCLC and a subset of non-SCLC. Previously, to understand how ASCL1 initiates tumorigenesis in pulmonary neuroendocrine cancer and identify the transcriptional targets of ASCL1, whole-genome RNA-sequencing analysis combined with chromatin immunoprecipitation-sequencing was performed with a series of lung cancer cell lines. From this analysis, we discovered that the gene SCNN1A, which encodes the alpha subunit of the epithelial sodium channel (αENaC), is highly correlated with ASCL1 expression in SCLC. The product of the SCNN1A gene ENaC can be pharmacologically inhibited with amiloride, a drug that has been used clinically for close to 50 years. Amiloride inhibited growth of ASCL1-dependent SCLC more strongly than ASCL1-independent SCLC *in vitro* and slowed growth of ASCL1-driven SCLC in xenografts. We conclude that SCNN1A/αENaC is a direct transcriptional target of the neuroendocrine lung cancer lineage oncogene ASCL1 that can be pharmacologically targeted with antitumor effects.

Translational Oncology (2018) 11, 292–299

Introduction

The majority of lung cancers are categorized as non–small cell lung cancer (NSCLC); the remaining 10% to 15% are classified as small cell lung cancer (SCLC), which is strongly associated with cigarette smoking. Pulmonary neuroendocrine (NE) lung cancers include SCLC and a subset, ~10%, of NSCLC [1]. Achaete-scute homolog 1 (ASCL1) is a basic helix-loop-helix transcription factor essential for the survival and progression ("lineage oncogene") of a large fraction of SCLC and NE lung cancer cells.

During development, ASCL1 regulates genes important for neurogenesis including those involved in Notch signaling and synapse formation [2–5]. Some other NE lung cancers are dependent on a related basic helix-loop-helix factor neuronal differentiation 1 (NeuroD1), also important at a later stage in neuronal development and for insulin gene transcription in pancreatic beta cells. Unlike

Address all correspondence to: Melanie H. Cobb, Department of Pharmacology or Jane E Johnson, Department of Neuroscience, 6001 Forest Park Blvd., Dallas, TX 75390-9041 or 9111, USA.
E-mail: melanie.cobb@utsouthwestern.edu
Received 31 August 2017; Revised 3 January 2018; Accepted 5 January 2018

1936-5233/18
https://doi.org/10.1016/j.tranon.2018.01.004

NeuroD1, ASCL1 is essential for development of pulmonary neuroendocrine bodies [6–8]. These cells are thought to be the cell of origin for SCLC [8–10].

SCNN1A encodes the α subunit of the epithelial sodium channel (ENaC), which is a heteromeric, sodium-permeable, non–voltage-sensitive ion channel expressed in epithelial tissues and a member of the Degenerin/ENaC family [11,12]. The channel consists of three homologous subunits: α, β, and γ. Based on structural information on a related channel, ENaC is thought to form a heterotrimer with the β and γ subunits [13]. Nevertheless, the ENaC α subunit expressed alone has been shown to carry current [14]. ENaC mediates the transport of luminal sodium ions across the apical membrane of epithelial cells. Thus, ENaC controls the reabsorption of sodium in kidney and colon and is important in liquid clearance by airway surface epithelial cells [15]. Due to the importance of ENaC in liquid clearance in the lung, inhibition of ENaC is being considered as an alternative strategy to increase airway surface fluid in cystic fibrosis [16,17].

ENaC activity is regulated primarily by its synthesis, trafficking, and turnover [11]. In the kidney, ENaC is under the control of hormones including the mineralocorticoid aldosterone and the antidiuretic hormone vasopressin, essential regulators of blood pressure [18,19]. ENaC is ubiquitinated by E3 ligases such as Nedd4-2 which promotes its degradation [20,21]. Aldosterone induces ENaC transcription and also suppresses ENaC degradation through a protein kinase–dependent pathway [21–23]. For nearly 50 years, ENaC has been inhibited clinically with orally effective potassium-sparing diuretics such as amiloride and its derivatives [11].

To develop new therapies for SCLC and other neuroendocrine lung cancers, we have been determining the role of targeting ASCL1 and NEUROD1 as lineage oncogenes [8,24,25]. Whereas ASCL1 and NEUROD1 can be genetically inhibited, the lack of pharmacological approaches has led us to start to interfere with direct transcriptional targets of these transcription factors that could be druggable. We found that SCNN1A is associated with ASCL1 expression in SCLC and that ASCL1, but not NeuroD1, binds to a region of the SCNN1A gene, consistent with a direct transcriptional role for ASCL1. In this study, we evaluated the possibility that ENaC could be a pharmacologically approachable therapeutic target in ASCL1-dependent SCLC.

Materials and Methods

Lung Cancer Cell Lines

Lung cancer cell lines were obtained from the Hamon Center for Therapeutic Oncology Research. The identity of all cell lines was verified by DNA fingerprinting using the Promega Fusion system which consists of 24 short tandem repeat markers. All cell lines were free from *Mycoplasma* contamination. H889 and other cell lines were grown in RPMI medium with 5% FBS. Human bronchial epithelial cells were immortalized (HBEC3KT) only or also transformed (HBEC3KTRL53) as described [26,27]. These cells were maintained in distinct media as described in the previous references.

Lentivirus-Mediated shRNA Knockdown

The shASCL1and cells lines were generated via infection of lentiviral shRNA vector pTY-shRNA-EF1a-puroR-2a-GFP plasmids as previously described [24]. The shRNA virus-expressing lung cancer cells were selected with 1 μg/ml puromycin for 4 days after 2 days of viral infection.

Immmunoblotting and Antibodies

Equal amounts of lysate proteins were resolved by polyacrylamide gel electrophoresis in the presence of sodium dodecyl sulfate and transferred to nitrocellulose membrane (Millipore). Membranes were blocked with LI-COR blocking buffer, and primary antibodies were incubated with membranes overnight. LI-COR fluorescent secondary antibodies were used at 1:15,000, and immunoblots were imaged and bands quantified using LI-COR Odyssey Infrared Imaging System. The following primary antibodies were used: rabbit anti-ERK1/2 (Y691 [28]); mouse ASCL1 (BD Biosciences); ENaC alpha subunit (H-95, Santa Cruz); cleaved poly-ADP-ribose polymerase (PARP) (Asp214, #9541S, Cell Signaling Technology).

Cell Viability Assay

A total of 2×10^3 cells were plated in 96-well dishes and treated with DMSO or increasing concentrations of amiloride. At 0 and 24 hours postplating, 20 μl of CellTiterBlue reagent (Promega) was added to each well for 1.5 hours at 37°C. Emission at 590 nm was measured after excitation at 560 nm using a Synergy 2 multimode microplate reader (BioTek) with Gen5 software. Data were plotted relative to emission at day 0.

Colony Formation Assay

Soft agar and liquid colony assays were as described previously [24]. Briefly, 2000 viable cells were suspended and plated in 0.37% Sea Kem agar (FMC, Philadelphia, PA) in RPMI 1640 medium supplemented with 20% of fetal bovine serum with or without 100 μM amiloride in triplicate in 12-well plates, and were layered over a 0.50% agar base in the same medium as the one used for suspending the cells. To measure the effect of amiloride, 100 μM was added to the agar base layer. The number of visible colonies (>0.2 μm colony diameter) was counted 5 weeks later.

Real-Time RT-PCR

Total RNA from cell lines was isolated with TRI Reagent (Invitrogen). cDNA was synthesized using iSCRIPT cDNA Synthesis Kit with 0.1 μg total RNA (Bio-Rad). The resulting cDNA served as template for quantitative PCR analysis with iTaq Universal SYBR Green Supermix (Bio-Rad); relative transcript levels were normalized to actin mRNA. Data were analyzed using Bio-Rad CFX Manager (version 3.0). Primers for specific genes are as follows: human Actin, 5'-AGGTCATCACTATTGGCAACGA-3' and 5'-CACTTCATGATGGAATTGAATGTAGTT-3'; human GAPDH, 5'-CTGGAGAAACCTGCCAAGTA-3' and 5'-TGTTGCTGTAGCCGTATTCA-3'; human ASCL1, 5'-CCCAAGCAAGTCAAGCGACA-3' and 5'-AAGCCGCTGAAGTTGAGCC-3'; human SCNN1A, 5'-TCTGCACCTTTGGCATGATGT-3' and 5'-GAAGACGAGCTTGTCCGAG-3'; human SCNN1G, 5'-GCACCCGGAGAGAAGATCAA-3' and 5'-TACCACCGCATCAGCTCTTTA-3'; human SCNN1D, 5'-AGGAGGCTCACCTGGTCAT-3' and 5'-TGTATCGGGCCAGAGAGTAGG-3'; human SCNN1B, 5'-AGACAACCACAATGGCTTAACA-3' and 5'-TGAGGCTACATAGTCTCATGGC-3'.

Xenografts

A total of 1 million H69-Luc cells were injected into the flank of 10 mice as described [29]. One mouse was omitted from the study due to leakage of tumor cells during injection. Tumor volume was monitored on days indicated in the figure. Amiloride was added to the drinking

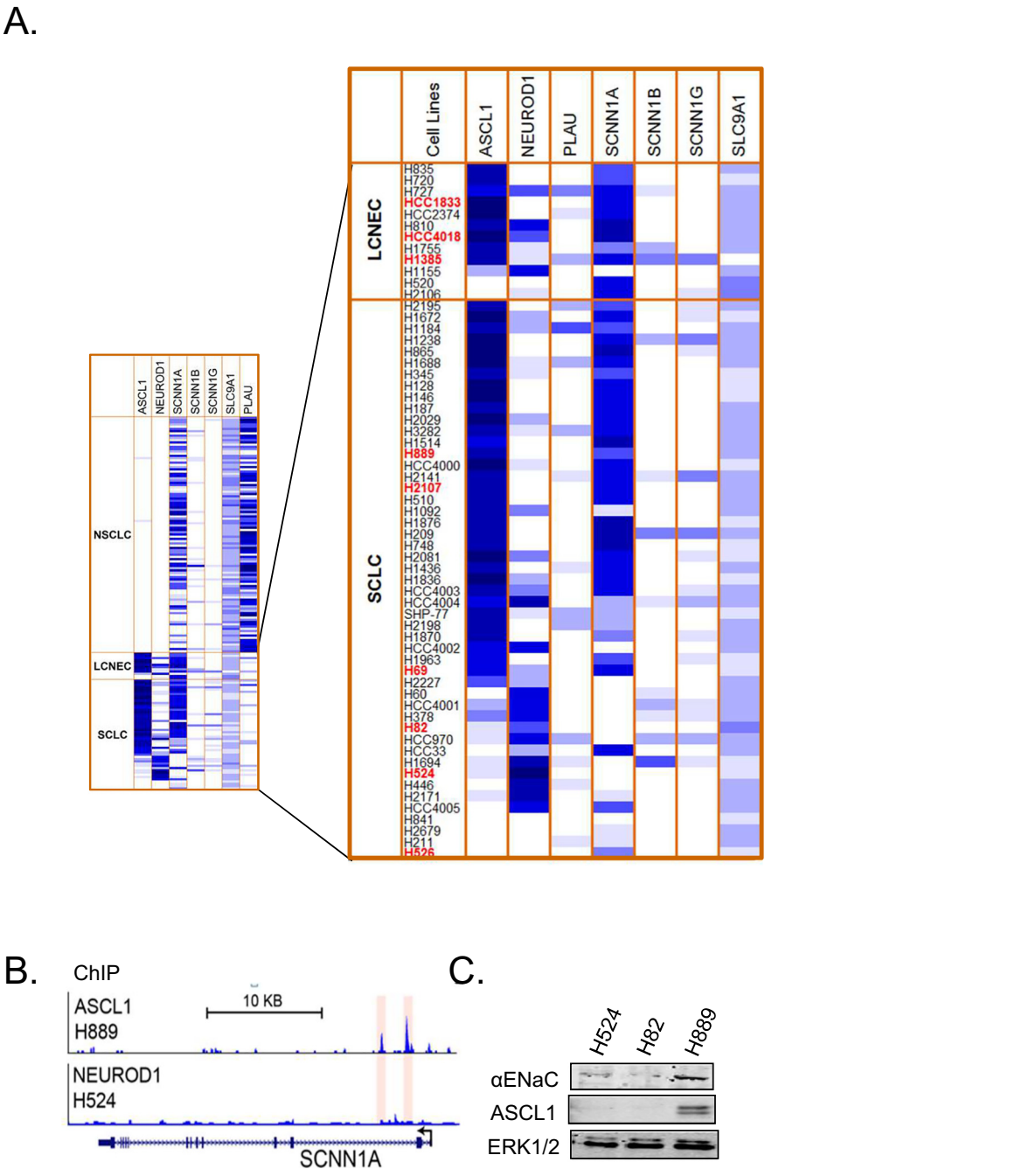

Figure 1. Among lung cancer cell lines, ASCL1-expressing cells also express αENaC, which is encoded by *SCNN1A*. (A) Expression of *ASCL1, NEUROD1 (ND1), SCNN1A, SCNN1B, SCNN1G, SLC9A1* (sodium-hydrogen exchanger, NHE1), and *PLAU* (urokinase-type plasminogen activator (uPA)) in lung cancer cell lines determined by RNA-seq (primary data will be available through the UT Southwestern lung cancer SPORE). Left panel shows data from a group of NSCLC and the neuroendocrine LCNEC and SCLC. Right is an expansion of data from LCNEC and SCLC showing cell line designations. Cell lines listed in red were used for experiments in this and subsequent figures. (B) ASCL1 ChIP-seq in H889 and NEUROD1 ChIP-seq in H524 show that ASCL1 but not NEUROD1 binds to an intronic region of the *SCNN1A* gene. (C) Western blots of ASCL1 and αENaC in three of the SCLC lines in (A). ERK1/2 blotted as loading controls.

water for five mice the second day after injection. On day 25, the experiment was terminated, and *P* values were calculated based on the difference in tumor volume at that time (*$P \leq 0.01$; Student's *t* test).

Immunofluorescence and image representation

Cells were washed twice with PBS and fixed, permeabilized, and blocked as indicated in Ref. [30]. Cells were then exposed to a 1:500 dilution of αENaC primary antibody (ThermoFisher PA1-920A) for 1 hour at room temperature with or without a 1:250 dilution of the antigenic/neutralizing peptide (ThermoFisher PEP-088; 0.5 mg/ml). Cells were exposed to the Alexa Fluor secondary antibody treatment (1:500) for 1 hour at room temperature with the addition of Alexa Fluor 647-phalloidin. Coverslips were mounted on DAPI-Fluoromount-G medium (SouthernBiotech). Images were

then obtained and deconvoluted as described in Ref. [30]. Z-stacks of deconvoluted images were opened in FIJI (ImageJ), and a middle plane was selected for representation.

Results and Discussion

Previously, we obtained ASCL1 and NeuroD1 chromatin immunoprecipitation-sequencing (ChIP-seq) and RNA-sequencing (RNA-seq) data from a series of lung cancer cell lines comprised of NSCLC, SCLC, and large cell neuroendocrine (LCNEC) lines including ASCL1^{high}NEUROD1^{low} SCLC lines H889 and H2107 and ASCL1^{low}NEUROD1^{high} SCLC lines H82 and H524 (Figure 1) [8]. From these data, we identified SCNN1A as a potential ASCL1 target gene based on its high expression in ASCL1-dependent SCLC (Figure 1*A*). ASCL1 binds within an intronic region of SCNN1A (Figure 1*B*), and its protein product ENaC was highly expressed in the ASCL1^{high}NEUROD1^{low} SCLC line H889 (Figure 1*C*). In contrast, ENaC was not detected in two ASCL1^{low}NEUROD1^{high} SCLC lines: H82 and H524.

Further evidence supporting a relationship between ASCL1 and SCNN1A came from examining their expression in a panel of lung cell lines. We found a parallel in mRNA expression of ASCL1 and SCNN1A in the NE-lung cancer cells but not in lung cancer cells lacking NE markers or the immortalized (HBEC3KT) or transformed (HBEC3KTRL53) HBEC lines [26,27] (Figure 2*A*). The cells expressing ASCL1 and SCNN1A did not express detectable amounts of mRNAs encoding other ENaC subunits SCNN1B, SCNN1G, or the related SCNN1D (Figure 2*B*). In fact, in an RNA-seq data set from a large panel of lung cancer cells including SCLC and NSCLC, we found that expression of the SCNN1B, D, and G subunits was low to undetectable. Significantly, we found that suppression of ASCL1 expression by infecting H889 cells with lentiviruses that stably expressed either of two shRNAs also reduced expression of SCNN1A (Figure 2, *C* and *D*), supporting the idea that SCNN1A is directly regulated by ASCL1. As expected, suppression of ASCL1 also resulted in increased apoptosis, revealed by enhanced cleavage of PARP (Figure 2*D*), consistent with many reports indicating that ASCL1 is required for growth of this tumor type [8,25,31–33].

Functional ENaC channels are usually expressed on the cell membrane. To determine whether this was the case in SCLC, we immunostained H889 with an antibody to the ENaC α subunit and found that the α subunit was detected on the plasma membrane in many cells (Figure 3, *top panels*). Intracellular staining was also noted in many of the cells. The overall intensity of staining was variable across the population, suggesting that some cells express much more α-ENaC than others. The antibody displayed reasonable specificity, as immunostaining was much reduced if the antigenic peptide to which the antibody was raised was included to compete with detection of the endogenous channel (Figure 3, *bottom panel*).

Amiloride directly blocks the epithelial sodium channel (ENaC), thereby inhibiting sodium reabsorption [11]. To determine if ENaC inhibition can mimic the ASCL1 loss-of-function effect to decrease cell viability, we tested the effects of amiloride on viability of H889 ASCL1^{high}NEUROD1^{low} and H82 ASCL1^{low}NEUROD1^{high} SCLC and immortalized HBEC3KT (Figure 4*A*). As amiloride concentration was increased, the viability of H889 cells dropped, but no effect on viability of H82 or HBEC3KT was observed. To obtain further evidence for an effect of amiloride, we treated NE-lung and immortalized nontransformed lung cells with the drug and blotted

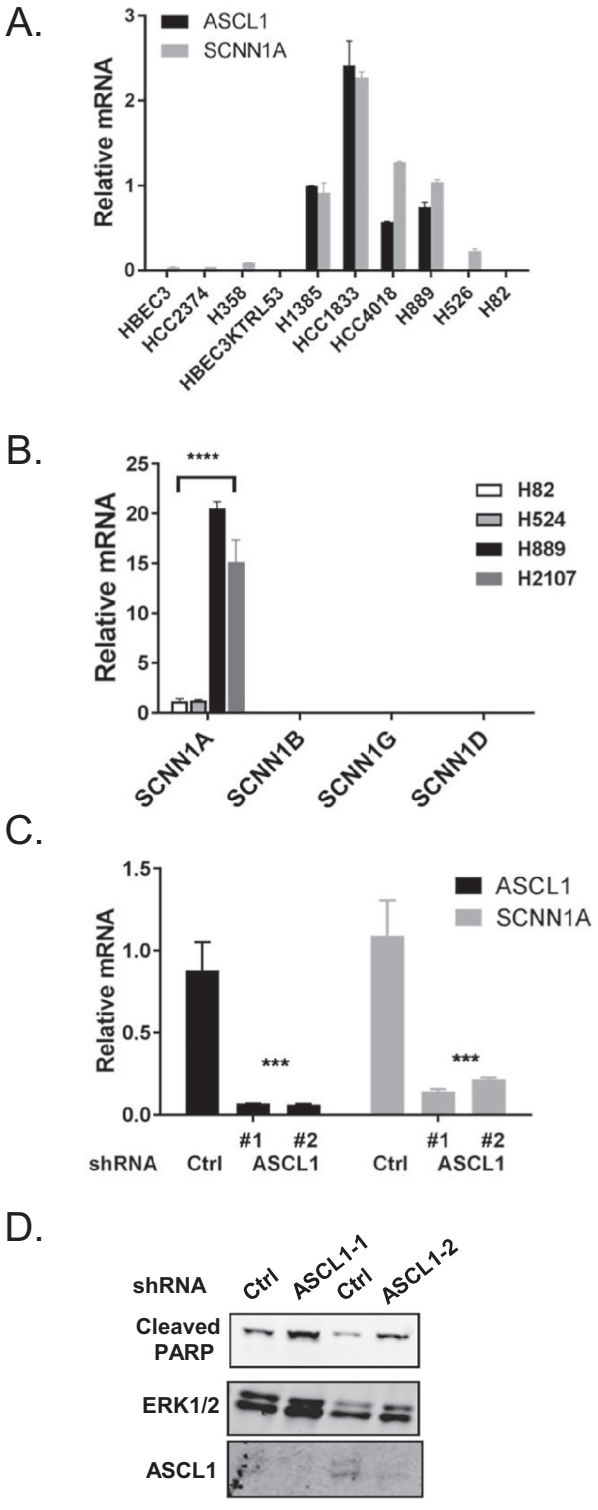

Figure 2. Expression of SCNN1A and other ENaC subunit mRNAs in lung cancer cells. (A) Expression of ASCL1 and SCNN1A in lung cancer cells and HBEC lines measured by quantitative RT-PCR. (B) Expression of the four ENaC subunits in four SCLC lines used for ChIP-seq and RNA-seq in a previous report [8]. (C) Two lentiviruses containing different shASCL1s were used to knock down ASCL1 expression in H889 cells. ASCL1 and SCNN1A expression was measured following ASCL1 knockdown. Error bars indicate standard deviation of three separate experiments. Significance was quantified by two-way ANOVA; *** = $P < 0.001$. (D) Lysate proteins were resolved by SDS-PAGE, immunoblotted for ASCL1, and cleaved PARP. Loading was normalized to ERK1/2.

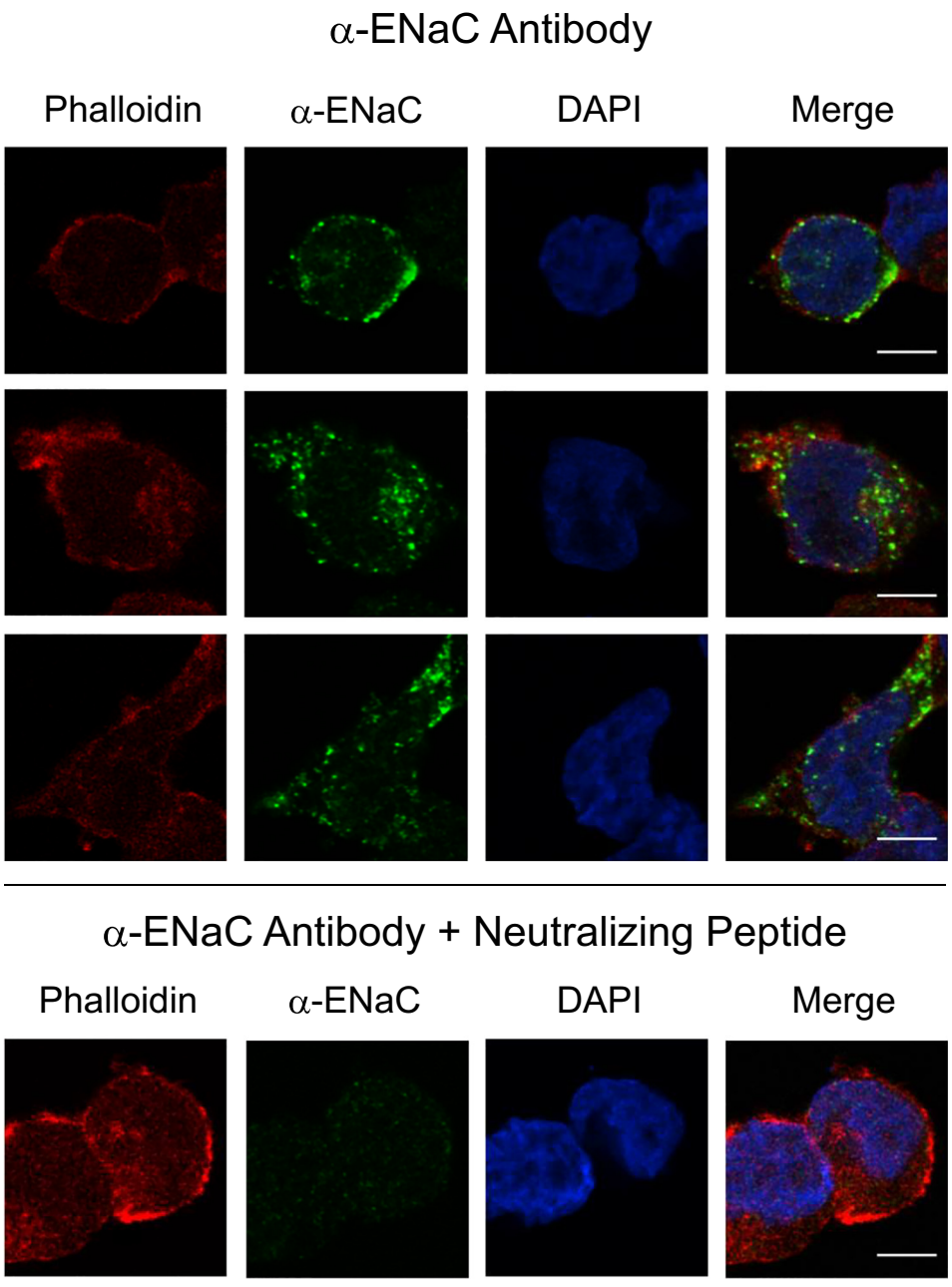

Figure 3. Glass coverslips in six-well dishes were coated with Cultrex diluted 1:20 with PBS. The excess was removed, and H889 cells were plated on the coverslips. The following day, cells were fixed and subsequently analyzed by immunofluorescence with an antibody to αENaC. Phalloidin was used to identify the cell periphery and DAPI to locate nuclei. (Top) Three sets of images are shown without the neutralizing peptide, and (bottom) one set of images is shown with the peptide. The signal was specific also based on minimal background staining by omitting the primary antibody (not shown). Scale bars, 5 μm.

cleaved PARP to assess apoptosis. Amiloride induced cleaved PARP in ASCL1^{high}NEUROD1^{low} SCLC H889 but not in the ASCL1-^{low}NEUROD1^{high} SCLC H82 (Figure 4*B*), the NSCLC cell line H358, or the immortalized HBEC3KT (Figure 4*C*).

The efficacy of amiloride was tested on colony formation in soft agar. Amiloride has an IC_{50} of approximately 100 nM for ENaC [11]. Thus, concentrations above the IC_{50} were tested. Two ASCL1^{low}NEUROD1^{high}, two ASCL1^{high}NEUROD1^{low}, and an ASCL1^{low}NEUROD1^{low} SCLC were treated with 50 μm amiloride. After 5 weeks, colonies were stained and counted (Figure 5*A*). Only the ASCL1^{high} SCLC displayed a significant reduction in colony number in the presence of amiloride. Two ASCL1^{high}NEUROD1^{low} NE-NSCLC lines, HCC1833 and HCC4018, were compared to the ASCL1- and NEUROD1-dependent lines, H889 and H82, with a higher amiloride concentration. Again, the three ASCL1-dependent lines, but not H82, displayed a substantial reduction in colony formation (Figure 5*B*).

Finally, we tested the effects of amiloride on the ASCL1-^{high}NEUROD1^{low} SCLC H69 grown as subcutaneous xenografts in immunocompromised mice. H69 cells were implanted in mice, and amiloride was placed in the drinking water beginning on the second day after implantation. In this subcutaneous xenograft model,

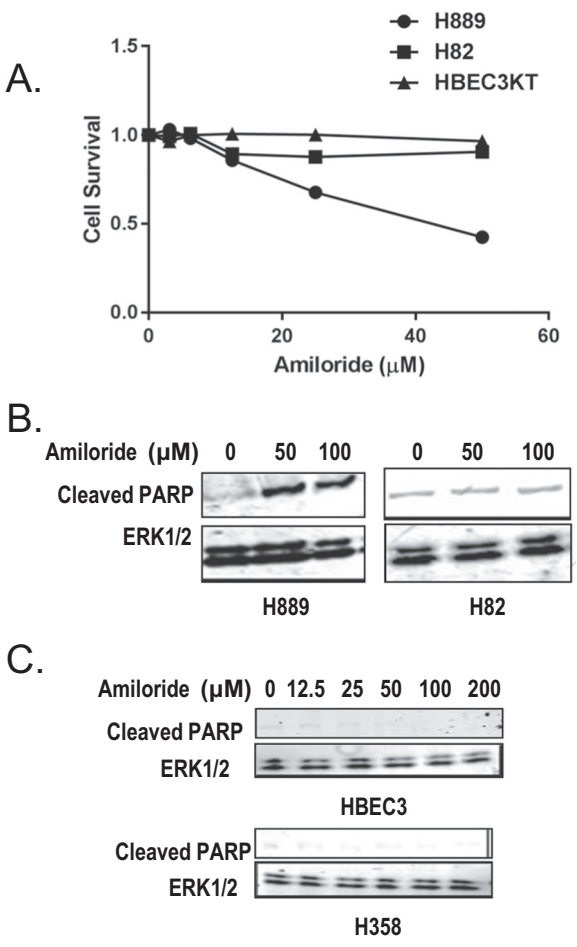

Figure 4. Effects of amiloride on SCLC, NSCLC, and immortalized human bronchial epithelial cells. (A) Viability of H889, H82, and HBEC3KT assayed as a function of amiloride concentration at 0 and 24 hours postplating. One of three similar experiments. (B) H889 and H82 were treated with the indicated concentrations of amiloride. Cleaved PARP was immunoblotted in cell lysates, and ERK1/2 were used as loading controls. (C) The immortalized HBEC3KT and NSCLC line H358 were exposed to a wider range of amiloride concentrations and processed for immunoblotting of cleaved PARP and ERK1/2 as in (B).

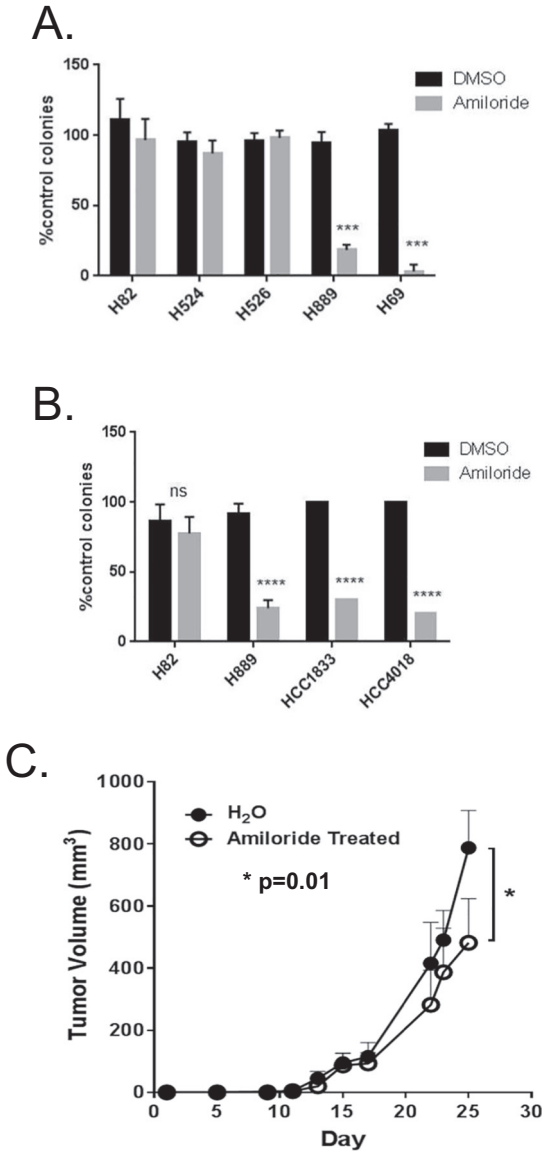

Figure 5. Amiloride inhibits soft agar colony formation and xenograft growth in ASCL1-driven NE lung cancer. A series of NE lung cancer cells was treated without or with 50 μm (A) or 100 μm (B) amiloride in soft agar assays. Graphs display colony counts relative to control colony number. Differences were analyzed for significance by two-way ANOVA; *** = $P<$ 0.001, **** = $P<$ 0.0001. (C) Xenograft growth over time in mice without or with amiloride in the drinking water for 25 days. Student's *t* test, $P = 0.01$

treatment with amiloride resulted in a reduced rate of tumor growth compared to the control (Figure 5*C*).

As an oral potassium-sparing diuretic, amiloride has previously been reported to have antitumor and antimetastasis functions in multiple studies in biochemical and cellular analyses and also in animal models [34,35]. *In vivo* studies showing that amiloride possesses antitumor properties appeared more than 30 years ago as reported by Sparks et al., who showed that amiloride inhibits growth of H6 hepatoma and also DMA/J mammary adenocarcinoma cells in xenografts in male A/J mice [36]. The rationale for testing amiloride at that time was the high intracellular concentration of sodium noted in cancer cell lines. We found that amiloride decreased growth rates in NE lung cancers that highly express ASCL1 but not in cells with low ASCL1 expression, suggesting that the effects of amiloride parallel ENaC expression.

Apart from its inhibition of ENaC, additional effects of amiloride have been found through other target or off-target effects. There are several reasons why at least some of these other reported targets are likely not responsible for the anti-SCLC effects described here. The most heavily characterized alternative target is the sodium-hydrogen exchanger 1 (NHE1; gene *SLC9A1* in Figure 1*A*), which is inhibited by amiloride at concentrations 10-fold above those required to block EnaC, within the range used for our studies. NHE1 is a primary cellular Na^+/H^+ antiporter and regulates intracellular pH. Upon activation, NHE1 activity may reverse the transmembrane pH gradient in transformed and malignant cells, lowering the extracellular pH, which makes a more favorable environment for extracellular matrix–degrading enzymes and proangiogenic factors [34]. Similar amounts of NHE1 mRNA (*SCL9A1*) are expressed in all of the cells tested, sensitive and insensitive alike. In particular, NHE1 mRNA is

similar in amount in the NEUROD1-dependent cells that are insensitive to amiloride (Figures 1*A* and 4*A*). The second alternative target is urokinase-type plasminogen activator (uPA; gene *PLAU* in Figure 1*A*) [34,37]. uPA becomes activated when binding to its cognate receptor the uPAR. uPA then cleaves cell surface-associated plasminogen to produce the serine protease plasmin, which activates extracellular proteases, e.g., matrix metalloproteinases, that degrade the matrix. uPA expression (gene *PLAU*) is barely detectable in the ASCL1- or NEUROD1-driven lines (Figure 1*A*). Amiloride derivatives also have some ability to interact with allosteric sites in certain G protein–coupled receptors such as the A2 adenosine receptor [38]. Like uPA, this receptor is expressed at a very low level in SCLC. Thus, it seems likely that these other targets contribute relatively little to the inhibitory actions of amiloride. Nevertheless, some off-target actions may contribute to the results we observe.

One remaining question is why only the ENaC α subunit is expressed at high levels in ASCL1-expressing cells. The other subunits are often absent from SCLC (Figure 1*A*). The ENaC α subunit expressed alone has been shown to carry current [14]; yet, it is usually coexpressed with other subunits and forms a heteromeric channel. Elevated expression of the β subunit has been suggested to cause dehydration of the lung surface [39]. Perhaps, this plays into the exclusive expression of the α subunit in many SCLC. Additionally, the ENaC α subunit can form a hybrid channel with ASIC1A, for example, an acidifying channel [40]. The formation of hybrid channels by the α subunit may bypass the need for expression of other ENaC proteins. Possible reasons for the importance of ENaC might involve changing intracellular pH or ion concentrations to protect ASCL1 from degradation or perhaps the channel is involved in masking the nonepithelial nature of the cells.

Conclusions

Taken together, these findings suggest that ENaC contributes to the growth of ASCL1-dependent NE lung tumors by a mechanism that is distinct from, or in addition to, those found in earlier studies. ENaC is expressed on the membrane, but exactly why this ion channel is required or what functions it is mediating to support tumor growth and survival are unclear at present. Nevertheless, ENaC may be a biomarker for ASCL1-dependent SCLC and may have value for future targeted therapies.

Acknowledgements

We thank members of the Cobb, Johnson, and Minna labs for comments and suggestions and Dionne Ware for administrative assistance.

Funding

This work was supported by grants from the Cancer Prevention and Research Institute of Texas jointly to M. H. C. and J. E. J. (RP140143) and by National Institutes of Health (R37 DK34128 to M.H.C. and P50CA70907 to J.D.M.), grants from the DOD PROSPECT and Longenbaugh Foundation to J. D. M., and the Robert A. Welch Foundation to M. H. C. (I1243). The final experiments were also supported by NCI U01 CA213338-01A1 to Minna, Johnson, Gazdar, and Cobb. The authors gratefully acknowledge assistance from the Harold C. Simmons Comprehensive Cancer Center core facilities supported in part by the National Cancer Institute (P30CA142543).

References

[1] Sun S, Schiller JH, Spinola M, and Minna JD (2007). New molecularly targeted therapies for lung cancer. *J Clin Invest* **117**, 2740–2750.

[2] Johnson JE, Birren SJ, and Anderson DJ (1990). Two rat homologues of Drosophila achaete-scute specifically expressed in neuronal precursors. *Nature* **346**, 858–861.

[3] Castro DS, Martynoga B, Parras C, Ramesh V, Pacary E, Johnston C, Drechsel D, Lebel-Potter M, Garcia LG, and Hunt C, et al (2011). A novel function of the proneural factor Ascl1 in progenitor proliferation identified by genome-wide characterization of its targets. *Genes Dev* **25**, 930–945.

[4] Guillemot F, Lo LC, Johnson JE, Auerbach A, Anderson DJ, and Joyner AL (1993). Mammalian achaete-scute homolog 1 is required for the early development of olfactory and autonomic neurons. *Cell* **75**, 463–476.

[5] Borromeo MD, Meredith DM, Castro DS, Chang JC, Tung KC, Guillemot F, and Johnson JE (2014). A transcription factor network specifying inhibitory versus excitatory neurons in the dorsal spinal cord. *Development* **141**, 2803–2812.

[6] Borges M, Linnoila RI, van de Velde HJ, Chen H, Nelkin BD, Mabry M, Baylin SB, and Ball DW (1997). An achaete-scute homologue essential for neuroendocrine differentiation in the lung. *Nature* **386**, 852–855.

[7] Ito T, Udaka N, Yazawa T, Okudela K, Hayashi H, Sudo T, Guillemot F, Kageyama R, and Kitamura H (2000). Basic helix-loop-helix transcription factors regulate the neuroendocrine differentiation of fetal mouse pulmonary epithelium. *Development* **127**, 3913–3921.

[8] Borromeo MD, Savage TK, Kollipara RK, He M, Augustyn A, Osborne JK, Girard L, Minna JD, Gazdar AF, and Cobb MH, et al (2016). ASCL1 and NEUROD1 reveal heterogeneity in pulmonary neuroendocrine tumors and regulate distinct genetic programs. *Cell Rep* **16**, 1259–1272.

[9] Sutherland KD, Proost N, Brouns I, Adriaensen D, Song JY, and Berns A (2011). Cell of origin of small cell lung cancer: inactivation of Trp53 and rb1 in distinct cell types of adult mouse lung. *Cancer Cell* **19**, 754–764.

[10] Park KS, Liang MC, Raiser DM, Zamponi R, Roach RR, Curtis SJ, Walton Z, Schaffer BE, Roake CM, and Zmoos AF, et al (2011). Characterization of the cell of origin for small cell lung cancer. *Cell Cycle* **10**, 2806–2815.

[11] Rossier BC (2014). Epithelial sodium channel (ENaC) and the control of blood pressure. *Curr Opin Pharmacol* **15**, 33–46.

[12] Hanukoglu I and Hanukoglu A (2016). Epithelial sodium channel (ENaC) family: phylogeny, structure-function, tissue distribution, and associated inherited diseases. *Gene* **579**, 95–132.

[13] Kashlan OB and Kleyman TR (2011). ENaC structure and function in the wake of a resolved structure of a family member. *Am J Physiol Renal Physiol* **301**, F684–F696.

[14] Canessa CM, Schild L, Buell G, Thorens B, Gautschi I, Horisberger JD, and Rossier BC (1994). Amiloride-sensitive epithelial Na+ channel is made of three homologous subunits. *Nature* **367**, 463–467.

[15] Matalon S, Bartoszewski R, and Collawn JF (2015). Role of epithelial sodium channels in the regulation of lung fluid homeostasis. *Am J Physiol Lung Cell Mol Physiol* **309**, L1229–L1238.

[16] Gianotti A, Melani R, Caci E, Sondo E, Ravazzolo R, Galietta LJ, and Zegarra-Moran O (2013). Epithelial sodium channel silencing as a strategy to correct the airway surface fluid deficit in cystic fibrosis. *Am J Respir Cell Mol Biol* **49**, 445–452.

[17] Donaldson SH and Galietta L (2013). New pulmonary therapies directed at targets other than CFTR. *Cold Spring Harb Perspect Med* **3**, 6.

[18] Bens M, Vallet V, Cluzeaud F, Pascual-Letallec L, Kahn A, Rafestin-Oblin ME, Rossier BC, and Vandewalle A (1999). Corticosteroid-dependent sodium transport in a novel immortalized mouse collecting duct principal cell line. *J Am Soc Nephrol* **10**, 923–934.

[19] Alvarez dlR and Canessa CM (2003). The role of the serum- and glucocorticoid-kinase in hormonal regulation of the epithelial sodium channel in A6 cells. *Am J Physiol Cell Physiol* **284**, C404–C414.

[20] Debonneville C, Flores SY, Kamynina E, Plant PJ, Tauxe C, Thomas MA, Munster C, Chraibi A, Pratt JH, and Horisberger JD, et al (2001). Phosphorylation of Nedd4-2 by Sgk1 regulates epithelial Na(+) channel cell surface expression. *EMBO J* **20**, 7052–7059.

[21] Bhalla V, Daidie D, Li H, Pao AC, Lagrange LP, Wang J, Vandewalle A, Stockand JD, Staub O, and Pearce D (2005). Serum- and glucocorticoid-regulated kinase 1 regulates ubiquitin ligase neural precursor cell-expressed, developmentally down-regulated protein 4-2 by inducing interaction with 14-3-3. *Mol Endocrinol* **19**, 3073–3084.

[22] De La Rosa DA, Li H, and Canessa CM (2002). Effects of aldosterone on biosynthesis, traffic, and functional expression of epithelial sodium channels in a6 cells. *J Gen Physiol* **119**, 427–442.
[23] Snyder PM (2002). The epithelial Na+ channel: cell surface insertion and retrieval in Na+ homeostasis and hypertension. *Endocr Rev* **23**, 258–275.
[24] Osborne JK, Larsen JE, Shields MD, Gonzales JX, Shames DS, Sato M, Kulkarni A, Wistuba II, Girard L, and Minna JD, et al (2013). NeuroD1 regulates survival and migration of neuroendocrine lung carcinomas via signaling molecules TrkB and NCAM. *Proc Natl Acad Sci U S A* **110**, 6524–6529.
[25] Augustyn A, Borromeo M, Wang T, Fujimoto J, Shao C, Dospoy PD, Lee V, Tan C, Sullivan JP, and Larsen JE, et al (2014). ASCL1 is a lineage oncogene providing therapeutic targets for high-grade neuroendocrine lung cancers. *Proc Natl Acad Sci U S A* **111**, 14788–14793.
[26] Ramirez RD, Sheridan S, Girard L, Sato M, Kim Y, Pollack J, Peyton M, Zou Y, Kurie JM, and DiMaio JM, et al (2004). Immortalization of human bronchial epithelial cells in the absence of viral oncoproteins. *Cancer Res* **64**, 9027–9034.
[27] Sato M, Vaughan MB, Girard L, Peyton M, Lee W, Shames DS, Ramirez RD, Sunaga N, Gazdar AF, and Shay JW, et al (2006). Multiple oncogenic changes (K-RAS(V12), p53 knockdown, mutant EGFRs, p16 bypass, telomerase) are not sufficient to confer a full malignant phenotype on human bronchial epithelial cells. *Cancer Res* **66**, 2116–2128.
[28] Boulton TG and Cobb MH (1991). Identification of multiple extracellular signal-regulated kinases (ERKs) with antipeptide antibodies. *Cell Regul* **2**, 357–371.
[29] Sato M, Larsen JE, Lee W, Sun H, Shames DS, Dalvi MP, Ramirez RD, Tang H, DiMaio JM, and Gao B, et al (2013). Human lung epithelial cells progressed to malignancy through specific oncogenic manipulations. *Mol Cancer Res* **11**, 638–650.
[30] Kankanamalage SG, Lee AY, Wichaidit C, Lorente-Rodriguez A, Shah AM, Stippec S, Whitehurst AW, and Cobb MH (2016). Multistep regulation of autophagy by WNK1. *Proc Natl Acad Sci U S A.* **113**, 14342–14347.
[31] Linnoila RI, Naizhen X, Meuwissen R, Berns A, and Demayo FJ (2005). Mouse lung neuroendocrine carcinomas: distinct morphologies, same transcription factors. *Exp Lung Res* **31**, 37–55.
[32] Jiang T, Collins BJ, Jin N, Watkins DN, Brock MV, Matsui W, Nelkin BD, and Ball DW (2009). Achaete-scute complex homologue 1 regulates tumor-initiating capacity in human small cell lung cancer. *Cancer Res* **69**, 845–854.
[33] Teicher BA (2014). Targets in small cell lung cancer. *Biochem Pharmacol* **87**, 211–219.
[34] Matthews H, Ranson M, and Kelso MJ (2011). Anti-tumour/metastasis effects of the potassium-sparing diuretic amiloride: an orally active anti-cancer drug waiting for its call-of-duty? *Int J Cancer* **129**, 2051–2061.
[35] Xu S, Liu C, Ma Y, Ji HL, and Li X (2016). Potential roles of amiloride-sensitive sodium channels in cancer development. *Biomed Res Int* **2016**, 2190216, https://doi.org/10.1155/2016/2190216.
[36] Sparks RL, Pool TB, Smith NK, and Cameron IL (1983). Effects of amiloride on tumor growth and intracellular element content of tumor cells in vivo. *Cancer Res* **43**, 73–77.
[37] Takahashi E, Abe J, Gallis B, Aebersold R, Spring DJ, Krebs EG, and Berk BC (1999). p90(RSK) is a serum-stimulated Na+/H+ exchanger isoform-1 kinase. Regulatory phosphorylation of serine 703 of Na+/H+ exchanger isoform-1. *J Biol Chem* **274**, 20206–20214.
[38] Massink A, Louvel J, Adlere I, van VC, Huisman BJ, Dijksteel GS, Guo D, Lenselink EB, Buckley BJ, and Matthews H, et al (2016). 5'-Substituted amiloride derivatives as allosteric modulators binding in the sodium ion pocket of the adenosine A2A receptor. *J Med Chem* **59**, 4769–4777.
[39] Livraghi-Butrico A, Wilkinson KJ, Volmer AS, Gilmore RC, Rogers TD, Caldwell RA, Burns KA, Esther Jr CR, Mall MA, and Boucher RC, et al (2017). Lung disease phenotypes caused by over-expression of combinations of alpha, beta, and gamma subunits of the epithelial sodium channel in mouse airways. *Am J Physiol Lung Cell Mol Physiol*, https://doi.org/10.1152/ajplung.00382.2017.
[40] Trac PT, Thai TL, Linck V, Zou L, Greenlee M, Yue Q, Al-Khalili O, Alli AA, Eaton AF, and Eaton DC (2017). Alveolar nonselective channels are ASIC1a/alpha-ENaC channels and contribute to AFC. *Am J Physiol Lung Cell Mol Physiol* **312**, L797–L811.